# Smectic and Cubic Mesophases of Alkylammonium Poly(vinylsulfonate)s

**Dimitris Tsiourvas and Constantinos M. Paleos**

*Institute of Physical Chemistry, NCSR "Demokritos", 15310 Aghia Paraskevi, Attiki, Greece*

**Antoine Skoulios***

*Groupe des Matériaux Organiques, Institut de Physique et Chimie des Matériaux, 23, rue du Loess, 67037 Strasbourg, France*

*Received June 29, 1999; Revised Manuscript Received September 29, 1999*

ABSTRACT: The thermotropic liquid crystal behavior of *n*-alkylammonium, *N*,*N*-dimethyl-*n*-alkylammonium, and quaternary *N*,*N*-dimethyl-*N*-cyanopropyl-*n*-alkylammonium poly(vinylsulfonate)s was investigated using differential scanning calorimetry, polarizing optical microscopy, and X-ray diffraction. All the hexadecyl and octadecyl derivatives exhibit a smectic B phase at low temperature and a smectic A phase at high temperature. The dodecyl and tetradecyl derivatives of the first two series exhibit a smectic A phase at all temperatures explored, from ambient up to thermal degradation. The dodecyl and tetradecyl derivatives of the third series show a smectic A phase at high temperature and, quite interestingly, an *Ia*3*d* body-centered-cubic phase at low temperature. The structure of the cubic phase consists of molecular bilayers bent according to Schoen's gyroid minimal surface. Sitting directly on the minimal surface, the polar heads of the molecules cover the same area in the cubic as in the adjacent smectic phase. The transition from cubic to smectic was briefly discussed.

## Introduction

The main characteristic of amphiphiles is their tendency to intramolecular microphase separation and spontaneous self-organization into well-defined supramolecular assemblies, such as micelles, vesicles, or lyotropic and thermotropic liquid crystals. A wide variety of monomer and polymer amphiphiles have been reviewed recently: soaps, protonated and quaternary long-chain ammonium salts, alkylated carbohydrates and polyols, polysoaps, amphiphilic polymers, and block copolymers.[1,2]

The thermotropic liquid crystal character of protonated long-chain ammonium salts with halide counterions was established long ago.[3] The role in the liquid crystal ordering of a variety of functional groups attached onto the ammonium cations, particularly of groups capable of interacting intermolecularly, was systematically studied in recent years.[4−6] The use of polyanions as counterions was first reported in the 1980s,[7,8] but the structure of the corresponding salts started being investigated systematically by X-ray diffraction only recently.[9−13] It was thus found that, in the case of *n*-alkylammonium polyacrylates, the liquid crystal structure depends on the particular amine employed: the dodecyl, didodecyl, and tetradecyl derivatives exhibit smectic A phases from room temperature up to thermal degradation, while the hexadecyl, octadecyl, and dioctadecyl derivatives exhibit ordered smectic B or E phases at low temperature and disordered smectic A phases at high temperature.[13] Likewise, in the case of quaternary alkyltrimethylammonium salts, it was found that, depending on the length of the alkyl chains and the nature of the polymer counterions used, several liquid crystal phases can be observed, among them liquid crystals with cubic symmetry.[12] Synthesized quite readily, such polymers have interesting properties, entering a variety of technological processes and formulations.[14]

In the present work, attention is focused on three further series of *n*-alkylammonium, *N*,*N*-dimethyl-*n*-alkylammonium, and quaternary *N*,*N*-dimethyl-*N*-cyanopropyl-*n*-alkylammonium salts bearing a poly(vinylsulfonate) counterion. The choice of these particular ammonium groups was merely intended to permit a rough estimate of the dependence of the liquid crystal structure on the bulkiness of the polar heads. Noted in the following as PV*n*, PD*n*, and PQ*n* ($n = 12, 14, 16, 18$ being the number of carbon atoms in the alkyl chains), these polymers have been characterized using polarizing optical microscopy, differential scanning calorimetry, and X-ray diffraction.

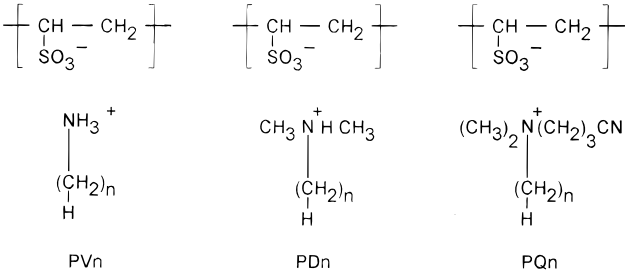


## Experimental Section

**Synthesis.** The poly(vinylsulfonic acid) sodium salt (Aldrich) used as starting material was isolated from its water solution by precipitation in methanol. Its degree of polymerization (DP ≅ 20) was measured by intrinsic viscosity in 0.346 M NaBr aqueous solution at 30 °C.[15] Its chemical composition was checked by elemental analysis [$C_2H_3O_3NaS$—Calcd: C, 18.5; H, 2.32; S, 24.6. Found: C, 17.2; H, 3.46; S, 21.2]; the discrepancy between the calculated and found values is, of course, related to the presence in the (short) polymer chains of (unsulfonated) end groups. The PV*n*, PD*n*, and PQ*n* ammonium salts were prepared in water by interaction of equimolar amounts of poly(vinylsulfonic acid) sodium salt with *n*-alkylammonium bromides (Aldrich), *N*,*N*-dimethyl-*n*-alkylammonium bromides (Hoechst), and *N*-cyanopropyl-*N*,*N*-dimethyl-*n*-alkylammonium bromides (synthesized in our labora-

* Author for correspondence.

10.1021/ma991051n CCC: $18.00 
Published on Web 11/10/1999

tory[4]). The resulting precipitates were filtered off, dissolved in chloroform, and reprecipitated in acetone for PV*n* and PQ*n* or in diethyl ether for PD*n*. The chemical structure was checked by FT-IR spectroscopy [data were recorded with a Nicolet Magna 550 spectrometer; the S=O stretching band of the sulfonic ion is shifted from 1038 $cm^{-1}$ for PVSANa to 1170−1190 and 1030−1032 $cm^{-1}$ for the ammonium salts; the $NH_3^+$ stretching band at 3250−3150 $cm^{-1}$ and the $NH^+$ stretching band at 3030 $cm^{-1}$ are closer to those of neutral amines than of their hydrobromide salts, as expected for PVSA−amine complexes: see ref 34] and confirmed by proton NMR spectroscopy [spectra in deuterated chloroform were recorded with a Bruker AC 250 spectrometer operating at 250 MHz; degrees of substitution higher than 0.95 were deduced from the integration of the peaks of the alkyl groups at $\delta$ = 0.85 ($CH_3$) and 1.25 ppm $(CH_2)_n$ and of the methylene and methine groups of the backbone at $\delta$ = 3.0−3.2 and 1.7−1.8 ppm]. Purity was checked by elemental analysis [PV12−$C_{14}H_{31}O_3NS$−Calcd: C, 57.3; H, 10.7; N, 4.8; S, 10.9. Found: C, 56.5; H, 10.7; N, 4.7; S,10.0. PV14−$C_{16}H_{35}O_3NS$−Calcd: C, 59.8; H, 11.0; N, 4.4; S, 10.0. Found: C, 58.5; H, 11.0; N, 4.3; S, 8.9. PV16−$C_{18}H_{39}O_3NS$−Calcd: C, 61.9; H, 11.2; N, 4.0; S, 9.2. Found: C, 60.8; H, 11.3; N, 4.0; S, 8.0. PV18−$C_{20}H_{43}O_3NS$−Calcd: C, 63.6; H, 11.5; N, 3.7; S, 8.5. Found: C, 62.1; H, 11.6; N, 3.6; S, 7.2. PD12−$C_{16}H_{35}O_3NS$−Calcd: C, 59.8; H, 11.0; N, 4.4; S, 10.0. Found: C, 59.0; H, 11.0; N, 4.1; S, 9.1. PD14−$C_{18}H_{39}O_3NS$−Calcd: C, 61.9; H, 11.2; N, 4.0; S, 9.2. Found: C, 60.8; H, 11.4; N, 3.8; S, 8.7. PD16−$C_{20}H_{43}O_3NS$−Calcd: C, 63.6; H, 11.58; N, 3.8; S, 8.5. Found: C, 62.5; H, 11.7; N, 3.7; S, 8.2. PD18−$C_{22}H_{47}O_3NS$−Calcd: C, 65.1; H, 11.7; N, 3.5; S, 7.9. Found: C, 63.9; H, 11.8; N, 3.4; S, 6.9. PQ12−$C_{20}H_{40}O_3N_2S$−Calcd: C, 61.8; H, 10.4; N, 7.2; S, 8.3. Found: C, 60.5; H, 11.0; N, 6.9; S, 7.4. PQ14−$C_{22}H_{44}O_3N_2S$−Calcd: C, 63.4; H, 10.6; N, 6.7; S, 7.7. Found: C, 62.2; H, 11.1; N, 6.6; S, 6.4. PQ16−$C_{24}H_{48}O_3N_2S$−Calcd: C, 64.8; H, 10.9; N, 6.3; S, 7.2. Found: C, 64.0; H, 11.2; N, 6.2; S, 6.5. PQ18−$C_{26}H_{52}O_3N_2S$−Calcd: C, 66.1; H, 11.1; N, 5.9; S, 6.8. Found: C, 64.9; H, 11.4; N, 5.8; S, 5.8. Degrees of substitution of the Na by ammonium cations were deduced from the N content of each compound: 0.94 for PD12, 0.95 for PD14, 0.96 for PQ12; 0.98 for PV12, PV14, PV18, PD16, PQ14, PQ16, and PQ18; 0.99 for PD18; and 1.00 for PV16].

**Characterization.** The thermal stability of the PV*n*, PD*n*, and PQ*n* salts was evaluated by isothermal and dynamical thermogravimetry using a TA TGA 2050 balance. Liquid crystalline textures were observed with a Leitz Wetzlar polarizing microscope equipped with a Linkam hot stage. Thermotropic polymorphism was investigated by differential scanning calorimetry with a TA DSC-10 instrument. The mesomorphic structures were studied by X-ray diffraction using a Guinier focusing camera (bent-quartz monochromator, Cu $K_{\alpha 1}$ radiation, powder samples in Lindemann capillaries, INSTEC hot stage, INEL CPS-120 curved position-sensitive detector).

## Results and Discussion

**Polymorphic Behavior.** The thermal stability of the ammonium salts synthesized was examined by thermogravimetry. Upon heating at 10 °C/min, the PV*n* and PD*n* derivatives started to degrade thermally at about 125 °C, while the PQ*n* compounds resisted thermal degradation up to about 160 °C. After a 4 h isothermal heating at 120 °C, the weight losses recorded were ranging from 0.5 to 3%: the shorter the chains and smaller the polar groups, the faster the degradation observed.

Investigated by optical microscopy, all the PV*n* and PD*n* compounds together with the quaternary PQ16 and PQ18 revealed themselves spontaneously birefringent, displaying well-developed oily streak liquid crystal textures in the whole range of temperatures explored, from ambient up to above thermal degradation. Characteristic of smectic structures, these textures were identical with those reported recently for the *n*-alkylammonium polyacrylate salts.[8,13] On the other hand, the PQ12 and PQ14 compounds showed themselves to be optically isotropic at low temperatures (their structure being cubic in symmetry as established below by X-ray diffraction). Above 200 and 130 °C, respectively, these compounds turned birefringent, displaying the same oily streak smectic textures as previously. Upon cooling, the transition back to the cubic state proceeded reversibly, but with a strong hysteresis; thus, below 130 °C, compound PQ14 became perfectly isotropic again, but rather slowly (after a half-hour annealing, for instance, at 105 °C).

**Table 1. Phase Transitions as Detected by DSC and X-ray Diffraction[a]**

| *n* | PV*n* | PD*n* | PQ*n* |
|---|---|---|---|
| 12 | A | A<br>$T_g \sim 51$ | Q [200] A |
| 14 | A<br>(B 37 A) | A<br>$T_g \sim 51$ | Q 122 A |
| 16 | B 54 A | B 45 A | B 27 A<br>(Q 99 A) |
| 18 | B 63 A | B 59 A | B 45 A |

[a] *n* is the number of carbon atoms in the alkyl chains; A, B, and Q stand for smectic A, smectic B, and *Ia*3*d* body-centered cubic; numerals represent peak values of transition temperatures in °C (the width and half-height of the B or Q to A peaks are of about 5 °C); $T_g$ are midpoint values of glass transition temperatures; data in parentheses correspond to observations during the first heating run only; data in brackets correspond to observations during thermal degradation.

Upon heating, the fluidity of the samples (except for PV12, which was fluid at room temperature) increased abruptly at a well-defined temperature below 65 °C, revealing either a glass transition (at 51 °C for PD12 and PD14, as confirmed by DSC, and at about 40 °C for PQ12 and PQ14, unconfirmed by DSC) or else a smectic B to smectic A phase transition (as confirmed by DSC and X-ray diffraction for PV14, and all the hexadecyl and octadecyl compounds cited in Table 1).

The polymorphic behavior of the PV*n*, PD*n*, and PQ*n* compounds was then investigated by differential scanning calorimetry in the range from room temperature up to 200 °C, beyond the onset of thermal degradation (Table 1). All the hexadecyl and octadecyl compounds were thus found to exhibit only one strong endotherm, corresponding to a first-order phase transition from smectic B to smectic A (as shown by X-ray diffraction). Located at 54 °C (61 J/g) for PV16, 63 °C (72 J/g) for PV18, 45 °C (55 J/g) for PD16, 59 °C (67 J/g) for PD18, 27 °C for PQ16, and 45 °C (45 J/g) for PQ18, these endotherms reflect mainly the melting of the alkyl chains. Upon cooling, the reverse transition back to smectic B proved extremely difficult to develop in general, the smectic A phase continuing to exist at room temperature for a long time, sometimes indefinitely. This strong hysteresis effect originates in the fact that a glass transition intervenes, during the transition process, severely slowing down the nucleation and growth kinetics of the smectic B phase. Figure 1 shows the hysteresis observed by X-ray diffraction with compound PV16. To illustrate the important part played by kinetics in the polymorphic behavior of the compounds under study, it is worth noting that, in the particular case of PQ16, the transition enthalpy measured during the first heating run was unexpectedly small (7 J/g); the reason was simply that, owing to the experimental

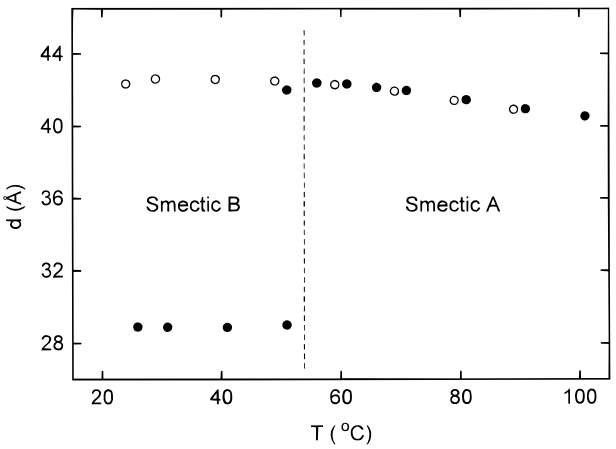


**Figure 1.** Temperature dependence of the smectic B and smectic A periods of the PV16 compound. Data of smectic B are represented by the four lowest-temperature closed circles, while data of smectic A are represented by the eight highest-temperature closed and all the open circles. Diffraction patterns (exposure times of 20 min) were recorded every 30 min during the stepwise heating or cooling of the samples.

conditions of synthesis, the PQ16 samples, normally in the smectic B state, were partly frozen in the smectic A or cubic state, as shown by X-ray diffraction and evidenced by the presence in the thermograms of an additional endotherm at 99 °C.

Of the dodecyl and tetradecyl compounds analyzed, the PQ*n* derivatives were found to exhibit only one rather weak (∼13 J/g) endotherm at 122 °C for PQ14 and 200 °C for PQ12 (beyond the onset of thermal degradation), corresponding to a first-order phase transition from cubic to smectic A. The PV*n* and PD*n* derivatives, on the other hand, displayed no phase transition at all, remaining in the smectic A state in the whole range of temperatures explored. For the sake of completeness, it is worth adding that, during the first heating run, compound PV14 exhibited a small endotherm at about 37 °C (2 J/g) due to the presence of traces of smectic B ordering as detected by X-ray diffraction.

**Smectic Structures.** The smectic liquid crystal phases detected by DSC and optical microscopy were fully confirmed and systematically analyzed by X-ray diffraction. The X-ray patterns recorded with the hexadecyl and octadecyl derivatives of the PV*n*, PD*n*, and PQ*n* compounds at low temperature, below the phase transitions detected by DSC (Table 1), are characteristic of smectic B structures. They contain up to three sharp equidistant reflections at small angles, consistent with a smectic layering, and a fairly narrow reflection at wide angles, indicative of a hexagonal packing of the linear alkyl chains.

Inspection of the experimental data shows that the cross-sectional area of the hexagonally packed alkyl chains, $\sigma = 19.5$ Å$^2$ for PV*n* or PD*n* and 19.9 Å$^2$ for PQ*n* (as deduced from the Bragg spacing of the wide-angle reflections at 4.11 and 4.15 Å, respectively), is very close to that found for smectic B phases in general: 19.9 Å$^2$, for instance, for alkylammonium polyacrylates[13] or 19.9 Å$^2$ for potassium soaps at low temperature in the presence of water.[16] Of about 80 Å, the correlation length of the hexagonal packing (as deduced from the width of the wide-angle reflections) is comparable to that measured with alkylammonium polyacrylates (70 Å)[13] but smaller than usually observed (150−200 Å) for low-molecular-weight smectic B phases.[17] On the other hand, the smectic periods measured at 25 °C (28.9 Å for PV16, 31.5 Å for PV18, 30.8 Å for PD16, 33.6 Å for PD18, 34.2 Å for PQ16, and 35.0 Å for PQ18) are very close to the length of the monomer repeat units in a fully extended, all-trans conformation (estimated by molecular modeling) and grows steadily from PV*n* to PD*n* to PQ*n* in proportion to the size of the polar groups. Clearly, the alkyl chains, standing upright in a head-to-tail interdigitated configuration, are arranged in single layers separated from each other by the negatively charged polymer backbones, as shown in Figure 2.

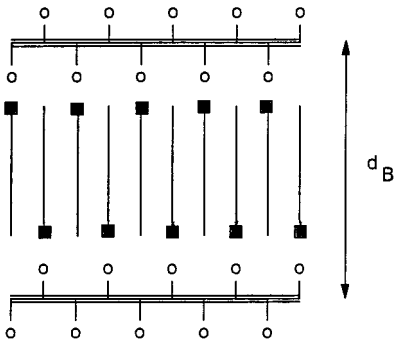


**Figure 2.** Schematic representation of the smectic B structure. For simplicity, ordered alkyl chains are depicted as straight lines, polymer backbones as straight triple lines, ammonium groups as closed squares, and sulfonic groups as open circles. The area covered in the smectic layers by the ammonium groups equals twice the cross-sectional area of the alkyl chains in an all-trans conformation ($S_B = 2\sigma$). The smectic period equals the length of the monomer repeat units ($d_B = L$).

The X-ray patterns obtained with the dodecyl and tetradecyl derivatives of the PV*n* and PD*n* compounds in the whole range of temperatures explored, from ambient to thermal degradation, and also with all the other compounds at temperatures above the phase transitions detected by DSC (Table 1), indicate the presence of smectic A structures. They contain up to three sharp equidistant reflections at small angles, typical of a smectic layering, and a broad wide-angle band at 4.5 Å, corresponding to the alkyl chains in a disordered, liquidlike conformation. It is worth noting that, due to an improved molecular ordering, the intensity of the small-angle reflections of PD12 and PD14 increases considerably above the glass transition at 51 °C, as already reported for the *n*-alkylammonium polyacrylates.[13]

Decreasing very slightly with increasing temperature ($\partial d/\partial T \sim -10^{-2}$ Å/°C), the periods measured for the smectic A phases grow linearly with the length of the alkyl chains (Figure 3), according to equations: $d$ (Å) $= 5.5_{\pm 0.5} + 2.27_{\pm 0.03}n$ for PV*n*, $d$ (Å) $= 9.4_{\pm 0.4} + 1.84_{\pm 0.02}n$ for PD*n*, and $d$ (Å) $= 13.8_{\pm 1.2} + 1.275_{\pm 0.07}n$ for PQ*n* (as deduced from a linear least-squares fit of experimental data at 70 °C). Exceeding the length of the monomer units (by as much as 45% for PV*n*, as shown in Figure 1), these periods suggest that, although jumbled together, the disordered alkyl chains have a tendency to arrange themselves in double layers (Figure 4).

The linear dependence of $d$ upon $n$ suggests at first sight that the lateral spreading of the molecules within the smectic A layers is independent of the length of the alkyl chains. From the slope of the straight lines and the known volume of one methylene group ($V_{CH_2} = 27.4$ Å$^3$ at 70 °C),[18] it is then easy to calculate the average

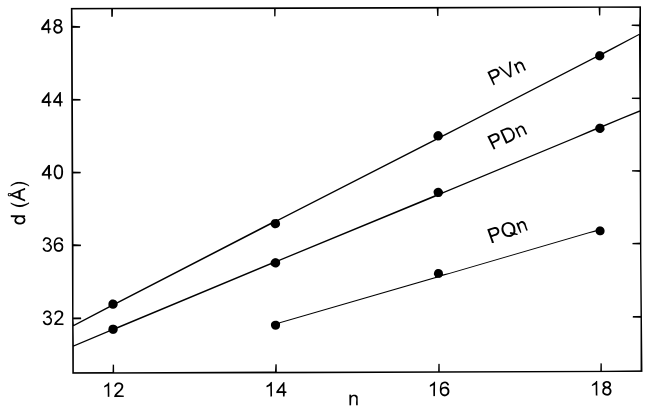


**Figure 3.** Variation of the lamellar period of the smectic A phases at 70 °C with the number *n* of carbon atoms in the alkyl chains.

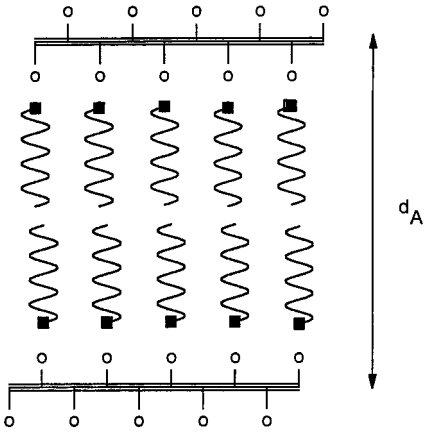


**Figure 4.** Schematic representation of the smectic A structure. For simplicity, disordered alkyl chains are depicted as wavy lines, polymer backbones as straight triple lines, ammonium groups as closed squares, and sulfonic groups as open circles. The area covered in the smectic layers by the ammonium groups equals the cross-sectional area of one molten alkyl chain ($\sigma < S_A < 2\sigma$). The smectic period exceeds the length of the monomer repeat units ($d_A > L$).

cross-sectional area of the disordered alkyl chains, using the equation $S = 2\ V_{CH_2}$/slope.[13] The value found for PV*n*, $S = 24.1 \pm 0.3$ Å$^2$, is much smaller than that (∼30 Å$^2$) of the *n*-alkylammonium polyacrylates[13] but close enough to the values generally quoted in the literature for smectic A structures (∼23 Å$^2$).[19] As for the values found for PD*n* and PQ*n*, $29.9 \pm 0.3$ Å$^2$ and $43.1 \pm 2.3$ Å$^2$, respectively, they are significantly larger on account of the larger size of the ammonium headgroups. The great influence of the size of these groups on the structural parameters is also visible in the thickness of the polar sublayers (5.5, 9.4, and 13.8 Å, as deduced from the *Y*-intercept of the *d* vs *n* straight lines of PV*n*, PD*n*, and PQ*n*). It is important to note in this connection that the molecular area of the headgroups of the PQ*n* compounds is appreciably larger in the smectic A (43.1 Å$^2$) than in the smectic B phase ($2 \times 19.9 = 39.8$ Å$^2$), showing clearly that their spontaneous cross-sectional area is also larger. As indeed expected, when released from the geometrical constraints imposed upon them by the ordering of the alkyl chains, the polar heads in the smectic A state are free to pack following their own nature and inclinations.

It is useful to close this section with a brief discussion of the smectic B to smectic A phase transition. From the experimental data collected in the present work, it

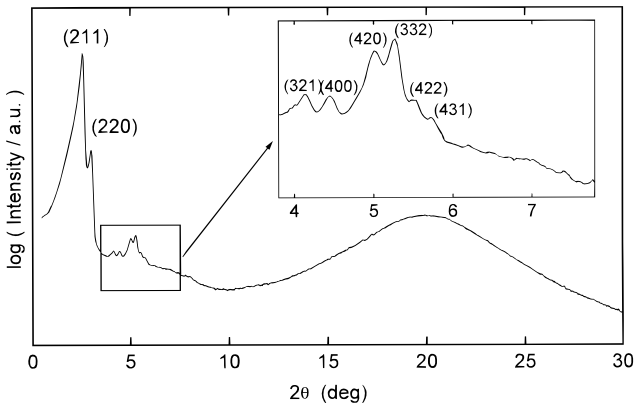


**Figure 5.** X-ray diffraction pattern of the *Ia*3*d* body-centered cubic phase of PQ12 at 20 °C. Data in parentheses are the Miller indices of the observed Bragg reflections.

**Table 2. X-ray Diffraction Data for PQ12 and PQ14 at 20 °C**[a]

| | | PQ12 ($a$ = 75.1) | | PQ14 ($a$ = 84.8) | |
|---|---|---|---|---|---|
| *hkl* | $h^2 + k^2 + l^2$ | $d_{calc}$ | $d_{obs}$ | $d_{calc}$ | $d_{obs}$ |
| 211 | 6 | 30.7 | 30.7 | 34.6 | 34.6 |
| 220 | 8 | 26.6 | 26.5 | 30.0 | 30.0 |
| 321 | 14 | 20.1 | 20.1 | 22.8 | 22.7 |
| 400 | 16 | 18.8 | 18.8 | 21.2 | 21.2 |
| 420 | 20 | 16.8 | 16.8 | 19.0 | 18.9 |
| 332 | 22 | 16.0 | 16.0 | 18.1 | 18.1 |
| 422 | 24 | 15.3 | 15.3 | 17.3 | 17.3 |
| 431/510 | 26 | 14.7 | 14.8 | 16.6 | 16.6 |

[a] $d_{obs}$ and $d_{calc}$ (in Å) are the observed and calculated spacings of the (*hkl*) small-angle reflections, and $a$ (in Å) is the cubic cell parameter.

emerges quite clearly that this transition coincides with an abrupt increase of the thickness of the smectic layers. Figure 1 shows as an example the temperature dependence of the smectic period across the smectic B to smectic A phase transition in the particular case of PV16. This effect reflects, of course, the volume expansion of the molecules at the melting of the alkyl chains but also reflects a crucial dependence on the variation of the molecular area of the polar heads. As it happens, this area decreases a great deal for PV*n* and PD*n*, passing from $2 \times 19.5 = 39.0$ Å$^2$ in the smectic B to 24.1 and 29.9 Å$^2$ in the smectic A phase, whereas it increases only slightly for PQ*n*, passing from $2 \times 19.9 = 39.8$ Å$^2$ to 43.1 Å$^2$. It is hence only very natural that the smectic layers increase so much in thickness for PV*n* and PD*n* (by 45 and 30%, respectively) and only so little for PQ*n* (by less than 3%).

**Cubic Structure.** The X-ray patterns recorded with PQ12 and PQ14 at low temperature, below the phase transitions detected by DSC (Table 1), contain a broad band at 4.5 Å related to the alkyl chains in a disordered conformation and quite a few sharp reflections in the small-angle region easily indexed as reflections from a cubic lattice (Figure 5, Table 2). Cubic structures have already been reported in the literature for other similar polymers, for instance for quaternary alkyltrimethylammonium polyacrylates,[12] but the one described in the present work is completely different. Instead of being face-centered, its Bravais symmetry is actually body-centered as established unambiguously by the presence of a (321) and a (420) Bragg reflection in the X-ray patterns. As for its space group symmetry, it is *Ia*3*d* as clearly deduced from the number of systematic absences (particularly of the (110), (200), and (310) reflections)

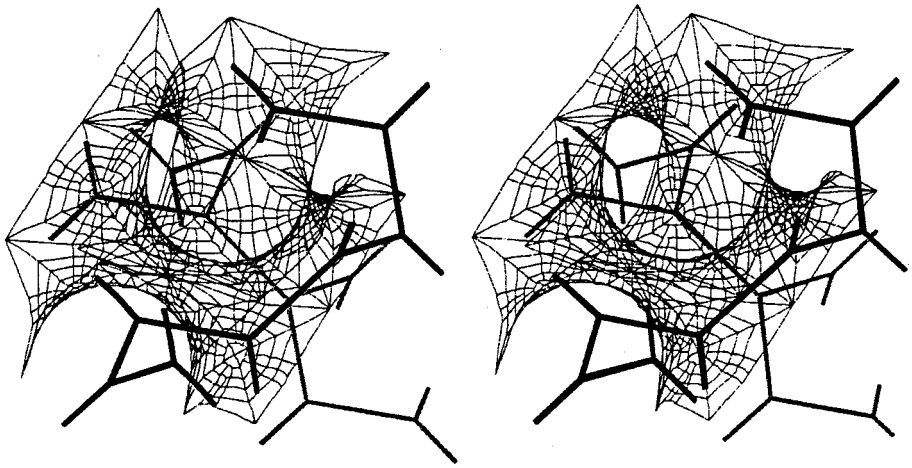

**Figure 6.** Stereoscopic view of a portion of the gyroid surface and of the full skeletal graph contained in one unit cubic cell.

and as supported by the intensity distribution of the observed reflections, which is similar to that reported in the literature for the strontium soaps[20] and the alkali metal dialkyl phosphate salts.[21]

Hardly depending on temperature ($\partial a/\partial T \cong -1.4 \times 10^{-2}$ Å/°C), the cubic cell parameters are $a = 75.1$ Å for PQ12 and 84.8 Å for PQ14. From the density of the two polymers ($1.17_4$ g/cm$^3$ for PQ12 and $1.15_4$ g/cm$^3$ for PQ14),[22] the number of monomer repeat units per cubic unit cell was found to be 770 for PQ12 and 1020 for PQ14, corresponding to some 40−50 macromolecules.

To get better insight into the structure of the *Ia*3*d* cubic phases observed, it is useful to recall briefly the concept of infinite periodic minimal surfaces[23] and specifically Schoen's gyroid surface extensively used to describe the *Ia*3*d* cubic phases of lyotropic[24] and thermotropic[25] liquid crystals, as well as of block copolymer systems.[26] By definition, the mean curvature of the minimal surfaces is zero everywhere [$H = (\kappa_1 + \kappa_2)/2 = 0$, $\kappa_1$ and $\kappa_2$ being the principal curvatures], while the Gaussian curvature is negative [$G = \kappa_1 \kappa_2 = -\kappa_1^2 \leq 0$]. Schoen's gyroid surface divides three-dimensional space into two distinct, equivalent, continuous, three-connected, and oppositely handed interpenetrating labyrinthine regions as depicted in Figure 6. The full set of the "axes" of the labyrinthine regions constitutes what is described to be the "skeletal graph" of the gyroid.[27] In lyotropic surfactant systems, as summarized by Hyde,[28] the gyroid surface describes the shape of one of the following types of layer: (i) curved bilayers of surfactant with the polar heads outside, separating the polar (water) regions in the two labyrinths; (ii) reversed curved bilayers of surfactant with the polar heads inside, separating the paraffin regions in the two labyrinths; (iii) monolayers of surfactant, separating the water and paraffin regions located separately in the two nonconnected labyrinths.

In thermotropic surfactant systems, that is, in the absence of water and oil segregating in the two labyrinths, only the first two models have to be taken into account. In the first model, the polar heads of the surfactant molecules are driven away from the gyroid surface and arranged in rods along the labyrinthine axes. As established experimentally, such is specifically the case of strontium soaps[20] and alkali metal dialkyl phosphates.[21] Quite interestingly, the cubic phases of these amphiphiles transform on heating into rodlike columnar phases, and the stacking period of the headgroups inside the rods keeps the same value across the

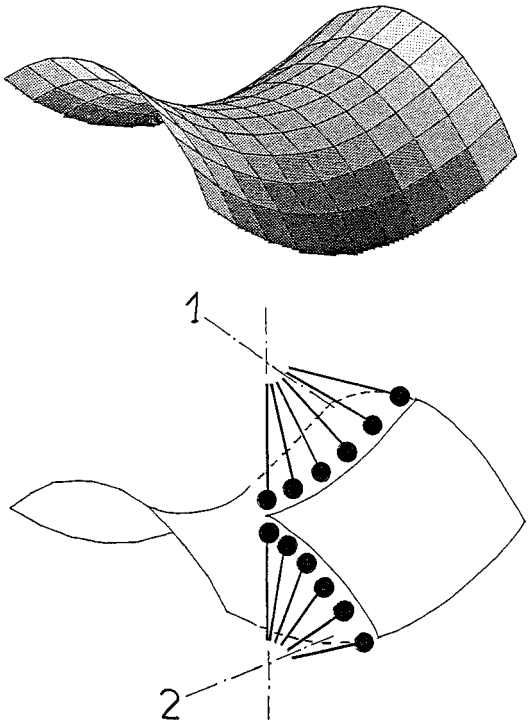


**Figure 7.** Schematic representation (top) of a small portion of the layerlike gyroid surface and (bottom) of two rows of molecules along the two lines of maximum curvature, with the polar heads sitting directly on the gyroid surface. The molecules on the upper face of the surface have their methyl terminal groups near axis 1 of the upper groove, while those on the lower face have their methyl terminal groups near axis 2 of the lower groove. Axes 1 and 2 are orthogonal to one another. In the case of a rodlike gyroid structure, the methyl terminal groups of the molecules are sitting directly on the gyroid surface while the polar heads are located in the immediate neighborhood of axes 1 and 2.

phase transition. In the second model, on the other hand, the polar heads are located directly at the gyroid surface itself, the disordered alkyl chains being now confined to the core of the labyrinths (Figure 7). To our best knowledge, no one definite example of amphiphile has been reported up to the present time, which exhibits such a layered arrangement of the molecules. It is true that the strontium soaps were revisited recently in this context; but, rather than to prove that their cubic structure was better described by the layer model, their reexamination was intended merely to show, in a concrete example, that the calculated intensity of the

Bragg reflections (in low-resolution X-ray diffraction patterns, where the detailed electron-density distribution is unimportant) was the same for both the rod and the layer model.[25] This result may also be deduced directly from Babinet's theorem,[29] which, applied to the present case, states that the diffraction pattern is the same no matter whether the scattering centers are located on the gyroid surface or on the labyrinthine axes.

In the present work, the rod model can hardly be used to describe the cubic structure observed. The polar groups are indeed too bulky to be wedged tightly in the narrow space round the axis of the rods and existing in too large quantities (a volume fraction of about 40−50%) to be surrounded evenly by the molten paraffin chains. More importantly, the polymer backbones, which are polydisperse and longer than each one of the rods of the "skeletal graph" of the gyroid, can hardly be taken to run uniformly along the labyrinthine axes without bifurcating at the triple junction points; topologically, they must hence be associated in even numbers and interwoven in a very special way, winding in three-dimensional space round the mutually orthogonal quaternary screw axes of symmetry of the *Ia*3*d* cubic crystal. Of course, such an arrangement would inevitably give rise to severe complications, not observed here, in the growth process of the cubic phase when generated by cooling from the high-temperature smectic A phase or by precipitation from a solution.

In contrast, the layer model, in which the polar heads are sitting directly on the gyroid surface, is far more convincing for several reasons. First, the cubic phase is followed, as it happens, by a smectic one at higher temperatures, which fact alone is a clear indication that a layered arrangement is perfectly suited to the shape of the molecules. Second, the molecular area of the polar heads at the gyroid surface of the cubic phase (45.3 Å$^2$ for PQ12 and 43.7 Å$^2$ for PQ14) is practically identical with that of the adjacent smectic A phase (43.1 Å$^2$), thus revealing explicitly a deep-seated analogy between the two phases. This molecular area is easily deduced from the number of monomer units inside one cubic unit cell and the total extension of the gyroid surface (3.091$a^2$).[30] Finally, the polar parts of the molecules being set in layers (and not in rods), the polymer backbones can arrange themselves without undue geometrical constraints, as easily in fact as in the adjacent smectic phases. It is useful to add immediately that the layered arrangement of the molecules is strengthened by the presence of cyano end groups in the polar heads, which, as established earlier for the crystal and smectic phases of *N*-cyanoalkyl-*N*,*N*-dimethyl-*n*-alkylammonium bromides,[4] compels the polar heads to join in pairs and so to pack in double layers covered on both sides by the molten alkyl chains of the molecules.

It is important to recall at this point that the planar bilayers of the smectic phases also correspond to minimal surfaces (zero mean curvature), but contrary to the gyroid bilayers, their Gaussian curvature is now zero everywhere. From a geometrical point of view, the cubic to smectic phase transition turns out therefore simply to amount to an abrupt vanishing of the Gaussian curvature of the bilayers at constant molecular area of the polar heads. The question arises at once of why in fact the planar molecular bilayers of the smectic phase should suddenly bend at the phase transition to adopt the gyroid shape of the cubic phase. Without entering into a detailed discussion of the thermodynamic potential of the phases, let us simply use the following geometrical argument. Differential geometry tells us that the molecular area $S(\xi)$ of the alkyl chains at a distance $\xi$ from the gyroid surface is related to the molecular area $S(0)$ of the corresponding polar groups sitting on the gyroid surface by $S(\xi) \cong S(0)[1 - |\langle G \rangle|\xi^2] < S(0)$.[30] In other words, the cross-sectional molecular area of the alkyl chains, which are driven away from the gyroid surface, is necessarily smaller than that of the polar heads on the surface: in the present case, by about 10% at a distance of 10 Å.[30] Apparently, therefore, the very existence of a cubic phase might be interpreted quite satisfactorily as resulting directly from an increased bulkiness of the polar headgroups with respect to the alkyl chains. This interpretation is perfectly consistent with the argument put forward by Charvolin and Sadoc, saying that, in the case of mismatch between the cross-sectional areas of the two constituent parts of an amphiphile, the molecular packing in planar layers is geometrically frustrated, inducing the formation of curved minimal surfaces.[32]

## Conclusion

The exchange of the cation of poly(vinylsulfonic acid) salts with long-chain alkylammonium, *N*,*N*-dimethylalkylammonium, and quaternary *N*,*N*-dimethyl-*N*-cyanopropyl-*n*-alkylammonium cations is a facile method for the preparation of a diversity of liquid crystal phases. By modifying the nature of the polar groups and changing the length of the alkyl chains, smectic A, smectic B, and *Ia*3*d* body-centered-cubic phases can be obtained. At high temperature, all the compounds synthesized in the present work, from dodecyl to octadecyl, produce smectic A liquid crystals independent of the chain length and bulkiness of the polar heads. At low temperatures, the longer alkyl chains have a tendency to arrange themselves in an orderly manner, inducing the formation of smectic B phases, while the shorter chains lead to the formation either of smectic A or *Ia*3*d* body-centered-cubic phases depending on the size of the polar heads. The structure proposed for the cubic phase consists of curved molecular bilayers located on a gyroid minimal surface, with the polar heads sitting directly on the surface.

A detailed analysis of the experimental data shows that, in the smectic B phases, the molecular area of the polar heads of the molecules is efficiently controlled by the cross-sectional area of the alkyl chains. These being arranged within the layers in a crystalline manner, the molecular area keeps the same value, $2 \times 19.6 = 39.2$ Å$^2$, for all the compounds studied. On the contrary, in the smectic A phases, where the alkyl chains are in a liquid state, the molecular area depends primarily on the size of the polar heads themselves, increasing from 24.1 Å$^2$ for PV*n* to 29.9 Å$^2$ for PD*n* and 43.1 Å$^2$ for PQ*n*. Furthermore, the molecular area increases slightly with temperature as indicated by the weak thinning of the smectic A layers upon heating and probably also with the length of the alkyl chains as observed in other similar cases.[32] It is of interest to remark that, at the smectic B to smectic A phase transition, the molecular area drops abruptly for the PV*n*'s and PD*n*'s, while it increases slightly for the PQ*n*'s. Apparently, the particular molecular area of the headgroups is smaller than the cross-sectional area of two crystalline alkyl chains in the first two series of compounds, while it is slightly larger in the last one.

Quite significantly, the cubic phases observed are obtained only with the PQ*n* compounds, that is, when the cross-sectional area of the headgroups goes slightly beyond what might be taken as the spontaneous cross-sectional area of the molten alkyl chains. In addition, they transform immediately into smectic phases either when the alkyl chains grow long enough or when the temperature is raised sufficiently, that is, when the cross-sectional area of the chains increases to match that of the polar heads. At any event, the molecular area in the cubic phase is comparable to that in the neighboring smectic phase, thus stressing the important part played by the packing of the polar heads inside the layers.

**Acknowledgment.** This work was carried out within the framework of the "Plato" bilateral cooperation program between Greece and France.

## References and Notes

(1) Paleos, C. M. *Mol. Cryst. Liq. Cryst.* **1994**, *243*, 159 and references therein.
(2) Tschierske, C. *Prog. Polym. Sci.* **1996**, *21*, 775 and references therein.
(3) Busico, V.; Corradini, P.; Vacatello, M. *J. Phys. Chem.* **1982**, *86*, 1033. Busico, V.; Cernicchlaro, P.; Corradini, P.; Vacatello, M. *J. Phys. Chem.* **1983**, *87*, 1631. Gault, J. D.; Gallardo, H. A.; Müller, H. J. *Mol. Cryst. Liq. Cryst.* **1985**, *130*, 163.
(4) Arkas, M.; Paleos, C. M.; Skoulios, A. *Liq. Cryst.* **1997**, *22*, 735.
(5) Paleos, C. M.; Arkas, M.; Seghroushni, R.; Skoulios, A. *Mol. Cryst. Liq. Cryst.* **1995**, *268*, 179. Paleos, C. M.; Arkas, M.; Skoulios, A. *Mol. Cryst. Liq. Cryst.* **1998**, *309*, 237.
(6) Alami, E.; Levy, H.; Zana, R.; Weber, P.; Skoulios, A. *Liq. Cryst.* **1993**, *13*, 201.
(7) Harada, A.; Nozakura, S. *Polym. Bull.* **1984**, *107*, 5300.
(8) Paleos, C. M.; Tsiourvas, D.; Dais, P. *Liq. Cryst.* **1989**, *5*, 1747.
(9) Ujiie, S.; Iimura, K. *Chem. Lett.* **1991**, 411. Ujiie, S.; Tanaka, Y.; Iimura, K. *Chem. Lett.* **1991**, 1037.
(10) Bazuin, C. G.; Tork, A. *Polym. Prepr.* **1996**, *37* (1), 776. Bazuin, C. G.; Brandys, F. A.; Eve, T. M.; Plante, M. *Macromol. Symp.* **1994**, *84*, 183. Bazuin, C. G.; Tork, A. *Macromolecules* **1995**, *28*, 8877.
(11) Tal'rose, R. V.; Kuptsov, S. A.; Sycheva, T. I.; Bezborodov, V. S.; Platé, A. *Macromolecules* **1995**, *28*, 8, 8689. Tal'rose, R. V.; Kuptsov, S. A.; Sycheva, T. I.; Shandryuk, G. A.; Platé, A.; Topchiev, A. V. In *Liquid Crystalline Polymer Systems, Technological Advances*; Isayev, A. I., Kyu, T., Cheng, S. Z. D., Eds.; ACS Symposium Series 632; American Chemical Society: Washington, DC, 1996; p 304.
(12) Antonietti, M.; Conrad, J. *Angew. Chem., Int. Engl. Ed.* **1994**, *33*, 1869. Antonietti, M.; Conrad, J.; Thünemann, A. *Macromolecules* **1994**, *27*, 6007. Antonietti, M.; Maskos, M. *Macromolecules* **1996**, *29*, 4199.
(13) Tsiourvas, D.; Paleos, C. M.; Skoulios, A. *Macromolecules* **1997**, *30*, 7191.
(14) Ober, K.; Wegner, G. *Adv. Mater.* **1997**, *9*, 17.
(15) Eisenberg, H.; Woodside, D. *J. Chem. Phys.* **1962**, *36*, 1844.
(16) Vincent, J. M.; Skoulios, A. *Acta Crystallogr.* **1966**, *20*, 432.
(17) De Gennes, P. G.; Prost, J. *The Physics of Liquid Crystals*; Clarendon Press: Oxford, U.K., 1993.
(18) Guillon, D.; Skoulios, A.; Benattar, J. J. *J. Phys. (Paris)* **1986**, *47*, 133.
(19) Skoulios, A.; Guillon, D. *Mol. Cryst. Liq. Cryst.* **1988**, *165*, 317.
(20) Spegt, P.; Skoulios, A. *Acta Cryst.* **1963**, *16*, 301. Luzzati, V.; Spegt, P. *Nature* **1967**, *215*, 701.
(21) Tsiourvas, D.; Kardassi, D.; Paleos, C. M.; Gehant, S.; Skoulios, A. *Liq. Cryst.* **1997**, *23*, 269. Paleos, C. M.; Kardassi, D.; Tsiourvas, D.; Skoulios, A. *Liq. Cryst.* **1998**, *25*, 267.
(22) The density was measured at 23 °C by determining the weight of a 5 mL volume-calibrated pycnometer filled with absolute ethanol in which about 1 g of polymer sample was immersed. Degassing was achieved by ultrasonication.
(23) Schoen, A. H. Technical Note NASA TN D-5541, 1970; *Not. Am. Math. Soc.* **1969**, *16*, 519.
(24) Scriven, L. E. *Nature* **1976**, *263*, 123.
(25) Clerc, M.; Dubois-Violette, E. *J. Phys. II* **1994**, *4*, 275.
(26) Hajduk, D. A.; Harper, P. E.; Gruner, S. M.; Honeker, C. C.; Kim, G.; Thomas, E. L.; Fetters, L. J. *Macromolecules* **1994**, *27*, 4063. Förster, S.; Khandpur, A. K.; Zhao, J.; Bates, F. S.; Hamley, I. W.; Ryan, A. J.; Bras, W. *Macromolecules* **1994**, *27*, 6922. Avgeropoulos, A.; Dair, G. J.; Hadjichristidis, N.; Thomas, E. L. *Macromolecules* **1997**, *30*, 5634.
(27) Grosse-Brauckmann, K. *J. Colloid Interface Sci.* **1997**, *187*, 418.
(28) Andersson, S.; Hyde, S. T.; Larsson, K.; Lidin, S. *Chem. Rev.* **1988**, *88*, 221. Hyde, S. T. *J. Phys. Chem.* **1989**, *93*, 1458.
(29) Lipson, H.; Cochran, W. *The Determination of Crystal Structures*; Bell and Sons: London, 1953.
(30) Differential geometry shows that the area $S(\xi)$ of a coordinate patch on a parallel surface standing at a distance $\xi$ from a reference surface is related to the area $S(0)$ of the corresponding patch on that reference surface by the relation $S(\xi) = S(0)[1 + 2\langle H\rangle\xi + \langle G\rangle \xi^2]$, where $\langle H\rangle$ and $\langle G\rangle$ are the average mean and Gaussian curvatures involved, respectively. For a minimal surface, $\langle H\rangle = 0$ and $\langle G\rangle < 0$, and $S(\xi) = S(0)[1 - |\langle G\rangle|\xi^2] < S(0)$.[28] Owing to the Gauss−Bonnet theorem, which relates the integral Gaussian curvature to the topological characteristics of surfaces, the average curvature of the gyroid in a *Ia*3*d* cubic structure is $\langle G\rangle = -8\pi/3.091a^2$, where $a$ is the cubic cell parameter.[31] In the present work, $a \approx 80$ Å, $\langle G\rangle \approx -10^{-3}$ Å$^{-2}$, and $S(\xi) \cong S(0)[1 - 10^{-3}\xi^2]$.
(31) Chung, H.; Caffrey, M. *Biophys. J.* **1994**, *66*, 377.
(32) Charvolin, J.; Sadoc, J. F. *J. Phys. (Paris)* **1987**, *48*, 1559.
(33) Arkas, M.; Yannakopoulou, K.; Paleos, C. M.; Weber, P.; Skoulios, A. *Liq. Cryst.* **1995**, *18*, 563.
(34) Bellamy, L. J. *The Infrared Spectra of Complex Molecules*, 3rd ed.; Chapman and Hall: London, 1975.

MA991051N